



## Functional amyloid materials at surfaces/interfaces

Cite this: *Biomater. Sci.*, 2018, **6**, 462 Chen Li,† Rongrong Qin,† Ruirui Liu, Shuting Miao and Peng Yang  \*

Received 4th December 2017,  
Accepted 29th January 2018

DOI: 10.1039/c7bm01124e

rsc.li/biomaterials-science

With the development of nanotechnology, functional amyloid materials are drawing increasing attention, and numerous remarkable applications are emerging. Amyloids, defined as a class of supramolecular assemblies of misfolded proteins or peptides into  $\beta$ -sheet fibrils, have evolved in many new respects and offer abundant chemical/biological functions. These proteinaceous micro/nano-structures provide excellent biocompatibility, rich phase behaviours, strong mechanical properties, and stability at interfaces not only in nature but also in functional materials, displaying versatile interactions with surfaces/interfaces that have been widely adopted in bioadhesion, synthetic biology, and composites. Overall, functional amyloids at surfaces/interfaces have excellent potential applications in next-generation biotechnology and biomaterials.

### 1. Introduction

Surface/interface science is a frontier field that is closely related to many high-tech applications such as electronics,<sup>1</sup> biotechnology,<sup>2,3</sup> and environmental science.<sup>4</sup> The building of functional and active surfaces/interfaces offers effective routes to enhance the bulk properties of materials or provide new functionality. Therefore, development of new functional on-demand surface/interface strategies for various substrates and purposes is crucial for material sciences and biotechnology. As one important example, in the last decade, mussel foot protein (MFP)-inspired 3,4-dihydroxyphenylalanine (DOPA) has offered a facile and green method for the modification of various substrates by complex surface polymerization chemistry.<sup>5</sup> However, some drawbacks are still unresolved, such as slow kinetics, dark coating colour, ill-defined polymerized products, material-dependent coating stability, and lack of activity at the liquid/liquid interfaces. Moreover, some natural polyphenols, such as tannins, readily bind to the surface and are cross-linked by coordination with iron ( $\text{Fe}^{3+}$ ); this provides another universal route of surface functionalization for different substances.<sup>6</sup> Similar to DOPA, characteristically dark colour and pH-dependent coating processes may be impediments to some applications. In addition to natural self-assemblies, chemical and physical methods, such as surface irradiation, layer-by-layer (LbL) assembly, and spin coating, are used for the modulation of functional surfaces.<sup>7</sup> However, these methods may only be suitable for particular materials/devices. In this

respect, studies on amyloids – another bio-inspired adhesive system – may create novel opportunities for surface/interface functionalization.

Amyloids were originally studied due to their roles in a series of neurological diseases. This term was first used in the medical literature by Rudolf Virchow to describe small deposits in the nervous system that could be stained by  $\text{I}_2$  and were therefore mischaracterized as starch-like materials.<sup>8</sup> However, amyloids have no connection with starch and are indeed fibrillar structures based on assemblies of proteins or peptides through the interaction of intramolecular and intermolecular  $\beta$ -sheets. X-ray diffraction patterns reveal that the spacing between the oriented  $\beta$ -strands in an amyloid is 4.8 Å, and the distance between the two parallel  $\beta$ -sheets in the amyloid is approximately 6 to 12 Å.<sup>9</sup> Based on their ordered structures, physical measurements of amyloids indicate that they are comparable to silk in terms of mechanical stiffness.<sup>10</sup> Conventionally, the deposition of amyloids in tissues and organs has been associated with various diseases, including Parkinson's disease, Alzheimer's disease and type II diabetes. The strong interactions between some amyloids and cell membranes are also responsible for a few types of toxic amyloids, especially pre-fibrillar structures.<sup>11</sup> On the other hand, a major class of amyloid structures without biological toxicity play functional roles in organisms, such as biosynthesis of melanin in mammals,<sup>12</sup> facilitation of information transfer<sup>13</sup> and controlled release of hormones.<sup>14</sup> Inspired by these natural functions, versatile amyloids are receiving continuing interest, and a number of remarkable applications have been developed.<sup>15</sup> Moreover, the interfacial behaviours of amyloids in some lower organisms and marine crustaceans reveal that amyloids can exhibit active behaviour at interfaces, such as the interactions between amyloid species and nanoparticles or cell mem-

Key Laboratory of Applied Surface and Colloid Chemistry, Ministry of Education, School of Chemistry and Chemical Engineering, Xi'an 710119, China.  
E-mail: yangpeng@snnu.edu.cn

† These authors contributed equally to this work.

**Table 1** Examples of functional amyloids with surface/interface functionality

Proteins	Interfacial properties	Functions	Ref.
ZPs	Mechanical properties	Amyloid protection	18,20
Hydrophobins (Fungi)	Interfacial assembly	Modulation of surface tension	19,33–37
Chaplins (Bacteria)	Interfacial assembly	Modulation of surface tension	19,46
CsgA and Tafi	Amyloid adhesion	Biofilm and surface functionalization	17,48–50,105
$\beta$ -Lactoglobulin	Interfacial activity	Stabilizer of liquid/liquid interface	93,94
Lysozymes	Amyloid adhesion	Surface functionalization	107, 108, 110–113,115,116

branes,<sup>16</sup> surface/interface functionalization,<sup>17</sup> protection from hazards,<sup>18</sup> and modulation of surface tension (Table 1).<sup>19</sup> Inspired by the versatile interactions between amyloids and surfaces/interfaces, active amyloids at surfaces/interfaces may exhibit better performance than existing surface chemical strategies, such as high transparency, excellent biocompatibility and strong activities at liquid/liquid interfaces, due to their proteinaceous motifs. Numerous efforts have been devoted towards high-performance engineering and functional materials; the fabrication of amyloid-based materials with additional chemical or physical properties often depends on complex designs of gene engineering and protein expression. Moreover, amyloid formation *in vitro* is often slow and induced by harsh conditions, such as low pH, high temperature and co-solvents. This review will focus on amyloid materials at surfaces/interfaces; we hope that this outline will encourage the fusion and development of amyloid-derived materials and surface/interface science.

## 2. Functional amyloids at surfaces/interfaces in nature

In nature, the role of amyloids is rather complex. They may be closely related to neurological disease, protein storage and bio-functional modulations. Amyloids as a functional material have been directly observed and are widespread in lower organisms, such as fungi, bacteria and invertebrates. One of the most important roles of amyloids in organisms is activating interactions at interfaces. We will summarize functional amyloids at surfaces/interfaces in nature in this section.

### 2.1 Amyloids are the major component of chorion

Chorion is the major component of the shells of insect and fish eggs. This proteinaceous shell provides excellent mechanical and physiological properties for protecting eggs from various hazards, including harsh physical conditions, proteases, and viruses. Moreover, 30% of chorion proteins produce amyloid fibrils under a variety of conditions, which suggests that the amyloids at the egg surface play an important functional role in protecting the oocyte from environmental hazards (Fig. 1a–c). About 200 proteins have been detected in silkworm chorion; these have been divided into two classes, A and B. Both A and B proteins can assemble into uniform amyloid-like fibrils in various conditions. On the other hand, the zona pellucida (ZP) surrounding the mammalian oocyte

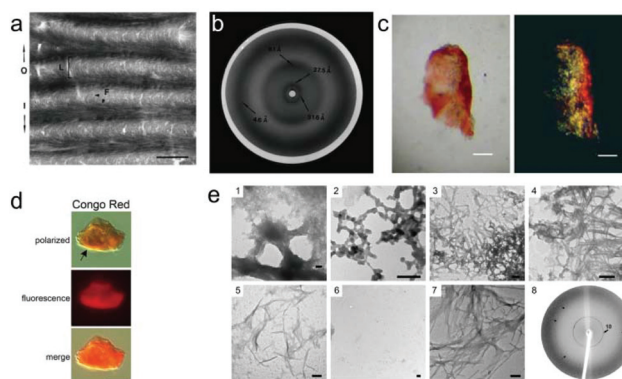


**Fig. 1** (a) Transmission electron microscopy images of an oblique section through the helicoid proteinaceous chorion of the silkworm *A. polyphemus*. Scale bar = 400 nm. (b) X-ray diffraction pattern from an almost flat fragment of a silkworm *A. polyphemus* chorion; the presence of reflections corresponding to periodicities of 4.6 and 9.1 Å suggests an abundance of  $\beta$ -sheets in the chorion proteins. (c) Bright field (left) and crossed polar (right) illumination of a portion of silkworm chorion from *Bombyx mori* stained with Congo red, scale bar = 400  $\mu$ m (a, b, c are reproduced from ref. 20, with permission from Wiley-VCH). (d) Congo red-stained ZP pellets showing yellow-green birefringence (arrow) when examined under polarizing light and bright red fluorescence when examined under UV light, scale bar = 10  $\mu$ m. (e) 1–5: TEM images of isolated ZPs which were digested with chymotrypsin. 6: Negative control in buffer containing chymotrypsin but not ZP. 7: A $\beta$  amyloid fibrils. 8: X-ray diffraction of mouse ZP (d and e are reproduced and adapted from ref. 29 with permission from Public Library of Science).

has also been proven to be a type of amyloid that plays a key role in the extracellular matrix (Fig. 1d and e). The ZP proteins have ZP polymerization domains that lead to protein fibril formation and assembly into the ZP matrix, which performs multiple functions during fertilization, including protection from polyspermy and cross-species fertilization.<sup>20</sup>

Amyloids in chorion were first found in fish and silkworm oocytes, which revealed their remarkable protective properties from environmental hazards. The electron image of a thin transverse section of chorion showed a lamellar ultrastructure of packed fibrils.<sup>21</sup> On the other hand, X-ray diffraction indicated that  $\beta$ -sheets were the dominant secondary structure.<sup>22</sup> Due to the fact that individual chorion proteins are difficult to purify in large amounts, several peptides that are considered to be the generic domains of the A and B families of chorions were synthesized to study their structural and assembly properties under different conditions.<sup>18</sup> A 51-residue peptide

(cA peptide) as a generic central domain of the A family was first synthesized by Benaki *et al.*;<sup>23</sup> this was proved to self-assemble into amyloid fibrils *in vitro* under a variety of conditions.<sup>24</sup> Additionally, some short peptides that are representative of parts of the central conservative domains of the A and B families of silkworm chorion proteins were designed and synthesized.<sup>25,26</sup> These peptides were also found to form amyloid fibrils by self-assembly mechanisms. These results strongly suggest that chorions are composed of self-assembled amyloid fibrils with protective properties at the surfaces of oocytes and embryos.

Similar to the chorion surrounding the oocytes in non-mammalian species, the ZP, which acts as an extracellular matrix surrounding mammalian oocytes and carries out multiple functions, is also a functional amyloid. Pioneering studies indicated that the mouse ZP is composed of three glycoproteins, ZP1, ZP2 and ZP3. In humans, a fourth protein that is highly similar to ZP1 is present and is called ZP4; the gene for ZP4 is not expressed in mice. All of these proteins have ZP polymerization domains that direct protein fibrillation and form the interfacial ZP matrix. The thick extracellular matrix plays important roles during oogenesis, fertilization and pre-implantation development.<sup>27</sup> It is noteworthy that the ZP polymerization domain has been found in hundreds of extracellular proteins with diverse functions in a wide variety of tissues and organisms. However, the mechanism of ZP polymerization and its role in gamete recognition remain unknown. Inspired by the functional amyloids in the epididymal lumen of mice and in the acrosomal matrix of sperm,<sup>28</sup> Egge *et al.* investigated the mouse ZP by collective evidence from conformation-dependent antibodies/dyes, X-ray diffraction, and negative stain electron microscopy, which suggested that amyloidosis may be a conserved mechanism for the ZP structure and its functions as an extracellular matrix.<sup>29</sup> Studies of the human ZP further supported that amyloidosis drives ZP matrix formation. Louros and co-workers designed and synthesized a series of “aggregation-prone” peptides corresponding to human ZP1, ZP2, ZP3 and ZP4. They found that these peptides self-assembled into fibrils in aqueous phase with distinct features, which revealed that the ZP domain of ZP proteins alone is responsible for the polymerization of ZP proteins and the formation of the ZP matrix.<sup>30,31</sup>

## 2.2 Amyloids for modulation of adhesion and surface tension

It has been suggested that amyloids are involved in the early evolution of proteins on prebiotic Earth.<sup>32</sup> Moreover, amyloids play a functional role in lower organisms, such as bacteria, fungi and insects. The unique mechanical and biological properties of amyloids enable their use as structural components for lower organisms. For example, for adaption towards moist environments, fungi must breach the air/water interface to grow in air (Fig. 2). Firstly, the water surface tension must be reduced before the hyphae can escape the aqueous phase. For this reason, most fungi can secrete amphipathic proteins known as hydrophobins to enable the growth of aerial struc-

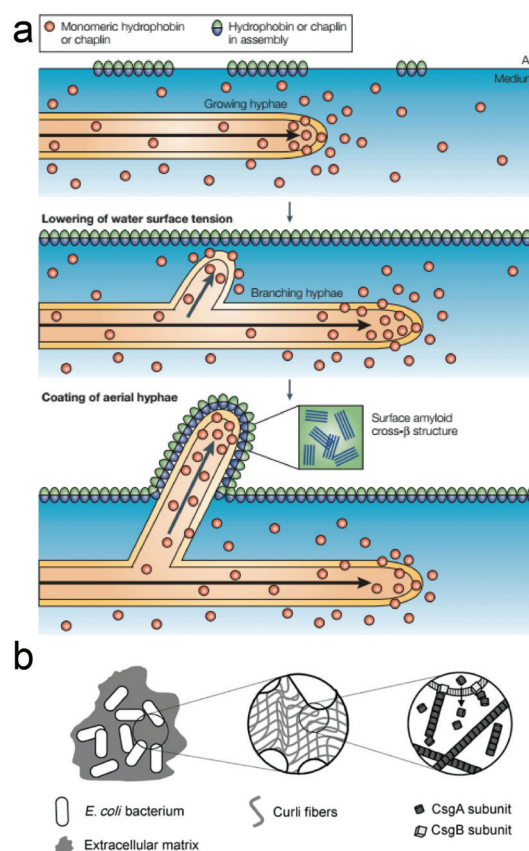


**Fig. 2** (a) The formation of amyloid structures enables streptomycetes and filamentous fungi to invade air; this membrane is composed of amyloid fibrils of hydrophobins and chaplins in filamentous fungi and streptomycetes, respectively. Aerial hyphae continue to secrete hydrophobins or chaplins, and these molecules assemble at the hyphal surface, conferring hydrophobicity (a is reproduced from ref. 19 with permission from Nature Publishing Group). (b) Schematic of the amyloidal Curli component of the bacterial extracellular matrix (b is reproduced from ref. 10 with permission from Wiley-VCH).

tures. The hydrophobins are a large family of small (7 to 9 kDa) secreted proteins that are unique to filamentous fungi.<sup>33</sup> The hydrophobins can reduce surface tension (*e.g.* from 72 to 24 mJ m<sup>-2</sup>) by assembly into monolayers at the air/water interface; these are known as rodlets (Fig. 2a).<sup>34</sup> On the other hand, hydrophobins can coat the surface of fungi to enable attachment to other hydrophobic substrates of hosts.<sup>35</sup> The rodlets exhibit many amyloid features, such as positive staining of ThT and Congo red,<sup>36</sup> typical X-ray diffraction patterns<sup>37</sup> and  $\beta$ -sheet-rich fibrillar structures; these typical features have led to various discussions of the assembly mechanism of hydrophobins. SC3 of *Schizophyllum commune* is a well-studied class I hydrophobin.<sup>33</sup> The self-assembly behaviors and conformational changes of SC3 monomers were investigated by de Vocht *et al.*;<sup>38</sup> the results showed that structural changes occurred upon assembly at both the air/water interface and the solid surface. The rodlets could not be removed by heating at 100 °C in 2% sodium dodecyl sulfate (SDS). The conformational changes of SC3 monomer led to a

transition from the  $\alpha$ -helical intermediate state to a stable  $\beta$ -sheet end configuration at the air/water interface,<sup>39</sup> and the amphipathic  $\alpha$ -helix formed as an anchor for binding to the solid surface.<sup>38</sup> Recently, Meister *et al.* used surface-specific vibrational sum-frequency generation spectroscopy (VSFG) to study the self-assembling mechanism of SC3 at the air/water interface.<sup>40</sup> An increased  $\beta$ -sheet-specific signal was observed, which proved the surface-driven self-assembly mechanism; also, the central  $\beta$ -barrel of SC3 remained intact and stacked into a larger-scale architecture of amyloid-like rodlets. Early studies on hydrophobins indicated that although the primary structures of hydrophobins are diverse, one main feature shared by recognized hydrophobins is the presence of 8 Cys residues that form four disulphide bridges (S-S bonds).<sup>33</sup> In order to investigate the role of these disulphide bridges in the assembly of hydrophobins, the S-S bonds were reduced with 1,4-dithiothreitol and the free thiols were blocked. The results indicated that the S-S bonds maintained the solubility of the hydrophobins in fungi cells and aqueous environments and prevented premature self-assembly.<sup>41</sup> In addition to SC3, the self-assembly behaviors of other class I hydrophobins have also been studied, such as DewA from *Aspergillus nidulans*,<sup>42</sup> EAS from *Neurospora crassa*<sup>43</sup> and Vmh2 from *Pleurotus ostreatus*.<sup>44</sup> These hydrophobins all exhibited similar assembly mechanisms and shared amyloid features with SC3, playing crucial functional roles in fungal reproduction and immune system evasion. In addition to fungi, the filamentous bacteria *Streptomyces coelicolor* can secrete a family of proteins that can form amyloid fibrils known as chaplins.<sup>45</sup> The chaplins family consists of eight proteins; ChpE and ChpH are secreted by submerged hyphae and can further assemble into insoluble fibrils at the air/water interface. The resulting structures can lower the surface tension and enable the hyphae to grow into air.<sup>46</sup>

A biofilm is an extracellular matrix (ECM) of bacteria composed of polysaccharides, proteins, nucleic acids and other biomolecular components; it is responsible for microbial adhesion to surfaces (Fig. 2b).<sup>47</sup> Curli and Tafi amyloid fibrils of *E. coli* and *Salmonella* spp. have been well studied for their functions in the attachment of bacteria to inert solid surfaces as well as their roles in biofilm formation.<sup>19</sup> The amyloid formation of Curli fibrils was firstly introduced by Chapman and his co-workers.<sup>48</sup> CsgA, a small protein with a molecular weight of 13 kDa, has been proven to be the major component of Curli fibrils. The intrinsically disordered CsgA can rapidly assemble into amyloid fibrils on the cell surface; this process promotes both cell-cell and cell-abiotic substrate interactions. On the other hand, the Tafi fibrils of *Salmonella* spp. have the same mechanisms of nucleation and aggregation as Curli fibrils; however, the Tafi fibrils prefer to interact with the cellulose of *Salmonella* spp., which is different from Curli.<sup>49</sup> DeBenedictis *et al.*<sup>50</sup> studied the adhesion of CsgA to both polar and nonpolar surfaces by atomistic simulations. They found that the polar residues and aromatic ring residues of CsgA could strongly interact with silica and graphene, respectively. Moreover, the good balance between the protein structure and non-covalent forces further enhanced the surface attachment. Generally

speaking, the bio-adhesion of amyloids contributes to both the toughness and adhesion of biofilms, leading to biofouling, bio-corrosion and bacterial colonization.<sup>51</sup> The discovery of functional amyloids in protective chorions, reproduction of fungi, and biofilms of bacteria revealed that the interfacial behaviours of amyloids play versatile roles in nature. Moreover, protein-based materials adopting amyloid-like conformations and aggregations have inspired the fabrication of functional materials at surfaces/interfaces, as discussed below.

### 3. Amyloids for surface/interface functionalization

Functional surfaces/interfaces with a variety of physical and chemical properties are significantly important in high-tech fields. Depending on the required interfacial properties, different methods have been developed, and convenient/environmentally friendly methods are urgently required. In this context, amyloids as biocompatible functional materials have presented excellent interfacial functions in synthetic systems. They have also inspired facile methodologies for the fabrication of novel interfacial materials and surface/interface functionalization.

#### 3.1 Interfacial behaviours of amyloid assemblies

Proteins sensitively interact with both biological and artificial interfaces, such as the assembly of membrane-bound  $\alpha$ -hemolysins into heptamers for transmembrane pores,<sup>52</sup> protein coronas for nanoscale objects,<sup>53</sup> and antifouling properties for artificial materials.<sup>54</sup> Also, as discussed in the previous sections, the formation of amyloids *in vitro* and *in vivo* can be greatly influenced by interfaces.<sup>55</sup> One of the most important hypotheses for amyloid toxicity is the strong interaction between cell membranes and amyloids (Fig. 3).<sup>11</sup> Amyloid formation can be accelerated or even catalysed by lipid membranes, as proven by numerous studies. At the initial stage, the anionic lipid headgroups can bind the basic

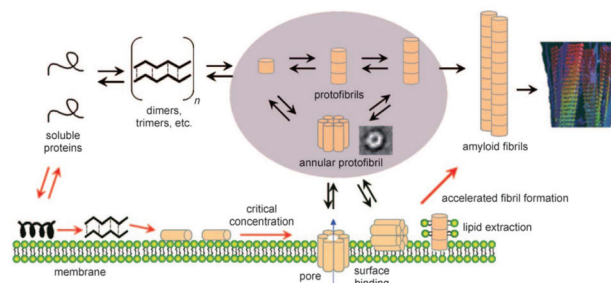


**Fig. 3** Interconnectivity between amyloid formation and membrane disruption. In the process of amyloid formation, the accumulation of proteins on the surface of the membrane induces their oligomerization into  $\beta$ -sheet aggregates. When a critical threshold concentration is reached, a transmembrane pore (annular protofibril) develops in the membrane and enables leakage of the membrane contents (reproduced from ref. 11 with permission from Wiley-VCH).

side chains of amyloid proteins. After further hydrophobic interaction with the buried acyl chains,<sup>56</sup> the proteins accumulate on the membrane surface and facilitate protein aggregation. Depending on the composition of the membrane and its chemical properties, various factors influence amyloid formation on the membrane surface, such as the surface charge of the membrane,<sup>57</sup> metal ions<sup>58</sup> and the protein-to-lipid ratio.<sup>59</sup> Although the mechanism of amyloid toxicity remains in debate, much evidence indicates that the interactions between amyloids and membranes can provoke permeabilization, which causes membrane thinning and ion leakage.<sup>60</sup> Visual evidence also proves the annular or ringlike structures of oligomeric amyloids by TEM and AFM, which supports the amyloid-pore hypothesis.<sup>61,62</sup> Amyloid formation can be influenced by different types of interfaces *in vitro*. Depending on the properties of the interfaces, unique amyloid assembly behaviours include acceleration or inhibition of amyloid fibrillation; also, the fine modulation of the morphologies of amyloid aggregations can be manipulated at interfaces. The interfacial fibrillations of a series of pathology-related proteins, such as A $\beta$ ,  $\alpha$ -synuclein, and insulin, were studied to achieve complete understanding of protein aggregation events *in vitro* as well as *in vivo*. Numerous studies have indicated that the surfaces of materials can affect amyloidosis and that proteins can adsorb onto surfaces to serve as reactive centers.<sup>63</sup> The absorption of proteins at the surface can increase the concentration of molecules locally, which appears to accelerate amyloidosis. Pandey *et al.*<sup>64</sup> studied the influences of surface hydrophobicity and roughness on insulin amyloidosis using mixed self-assembled monolayers of amine- and octyl-silanes. Both the functional groups and topography determined the lag phase of amyloid formation. Keller and his co-workers<sup>65</sup> fabricated ultrasubsmooth hydrocarbon films grown on ion-beam-modified mica surfaces with varying hydrophobicity. On these surfaces, without the effects of chemical composition or topography of the surfaces, the influence of the surface hydrophobicity on islet amyloid polypeptide (IAPP) assembly was investigated. The results showed that the strong electrostatic interactions between the monomers and the hydrophilic surface induced faster formation of amyloids than hydrophobic surface interactions. Shezad *et al.*<sup>66</sup> used polystyrene coatings and microparticles with varying roughnesses to study the effects of surface roughness on A $\beta$ <sub>42</sub> fibrillation. The results showed that rough surfaces heavily limited or even blocked the diffusion of peptides and inhibited fibrillation. This behaviour was also studied by Shen *et al.*,<sup>67</sup> who investigated the mobility of A $\beta$ <sub>42</sub> precursor on polymer surfaces with different hydrophobicities. Although the surface properties could increase the concentration of weakly adsorbed monomers, sufficient mobility of the adsorbed monomers may exert significant adverse effects. Therefore, a balance between the transient concentration and the mobility of the peptide precursor is critical for fibrillation. Growing evidence has revealed that the surface heavily influences both the kinetics of amyloid formation and the morphology of amyloid aggregates. Gao *et al.*<sup>68</sup> fabricated *N*-isobutyryl cysteine (NIBC)-enantiomer-modified ultra-flat

gold substrates; it was found that the surface chirality dominated the amyloid assembly of A $\beta$ (1–40) at low concentrations that were far below the CMC. They further showed that the D-surface induced rod-like amyloid aggregates and the L-surface and L + D surface induced ring-like aggregates. According to characterization by AFM-TERS (tip-enhanced Raman spectroscopy), Young's modulus, QCM (quartz crystal microbalance), and a molecular docking model, they proposed that electrostatic interactions and chiral recognition sites contribute to this behaviour. All of these principles can offer future guidance for both the mechanism of amyloid formation and the construction of functional amyloids at a surface.

Two-dimensional (2D) materials, such as graphene, graphene oxide (GO) and molybdenum disulphide (MoS<sub>2</sub>), have a significant impact on various applications, ranging from medicine and electronics to materials.<sup>69</sup> 2D materials can offer much larger liquid/solid interfaces when they are dispersed in aqueous phase, which has a strong influence on amyloid formation.<sup>70,71</sup> Regarding solid surfaces, a series of groups reported that graphene and GO can inhibit amyloid formation of various proteins, ranging from intrinsically disordered A $\beta$  to stable globular human serum albumin (HSA).<sup>72–76</sup> The combination of electrostatic interactions, hydrogen bonding, and van der Waals and hydrophobic interactions lead to the strong binding affinity between GO and proteins, which formed coronas around the GO. Although the absorption of proteins at the GO surface enhances the interfacial concentration of the protein, the intrinsic properties of GO inhibit amyloid formation because the steric repulsion and strong protein-GO interactions prevent interactions between the protein molecules;<sup>72,75</sup> also, the abundant hydrophobic  $\pi$  regions of GO can inhibit the transition of peptides from  $\alpha$ -helices to  $\beta$ -sheets.<sup>76</sup> Similar behaviour was observed using WS<sub>2</sub> nanosheets.<sup>77</sup> However, the different chemical properties of 2D materials can also provide alternative paths for amyloidosis. Qing *et al.*<sup>78</sup> fabricated cysteine enantiomer-modified GO to study how the surface chirality of GO influences the amyloid formation of A $\beta$ <sub>40</sub>. The results showed that R-cysteine modification suppressed fibrillation, while S-cysteine promoted this process. It was thus proven that the surface chirality greatly affected the transition from  $\alpha$ -helices to  $\beta$ -sheets, which presents a new perspective to understand how the surface chirality of nanoscale objects participates in amyloid formation. In addition to solid surfaces, air/water interfaces can also trigger amyloid formation. The surfactant-like properties of peptides leads to the absorption of peptides at the air/water interface by displacing weakly bound water molecules.<sup>79</sup> Moreover, the peptides are not only concentrated at the air/water interface, but also adopt preferred orientations and conformations to favour fibril formation.<sup>80,81</sup> Therefore, the presence of an air/water interface also plays multiple roles in amyloid-like protein aggregation, such as primary and secondary nucleation (Fig. 4).<sup>82</sup>

### 3.2 Amphiphilic amyloids at liquid/liquid interfaces

The adsorption of proteins at an interface can improve its interfacial properties, such as its foaming and emulsifying per-

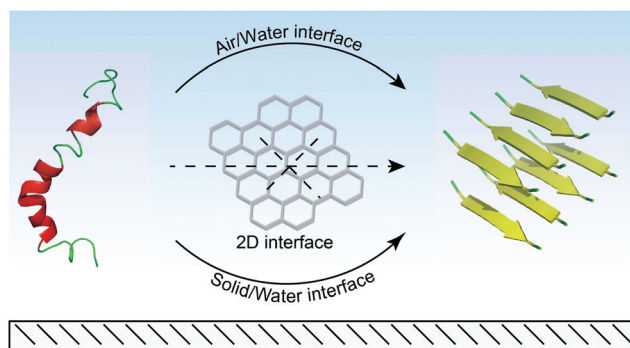


**Fig. 4** Amyloidosis of proteins and peptides can be accelerated by air/water or solid/water interfaces and inhibited by interfaces of 2D materials.

formance.<sup>83</sup> In addition to the interactions between proteins and liquid interfaces, such as electrostatic, hydrophobic, and van der Waals forces, the modification of proteins through chemical or physical methods can improve their interfacial properties due to the increase of hydrophobicity or the high surface affinity of large aggregated protein colloids.<sup>84,85</sup> In this regard, amyloid assemblies with regular micro/nano-structures can offer further geometrical constraints at the surface/interface. This combination of the benefits of proteins and amyloid particles exhibits a highly stabilizing effect at the liquid/liquid interface. These studies introduce new strategies for the fabrication of emulsions, protein capsules, droplets and microgels,<sup>86,87</sup> etc. In the formation of amyloid fibrils, the exposure of hydrophobic residues can induce nucleation and promote the formation of fibrils with a high aspect ratio. The interfacial properties and interfacial shear rheology of a 1D aggregation of  $\beta$ -lactoglobulin were firstly studied by Jung *et al.*<sup>88</sup> Their results showed that the surface tension at the air/water interface in the presence of  $\beta$ -lactoglobulin fibrils decreased more rapidly than that of the native monomer system. Interfacial tension measurements at the water/oil interface showed significantly faster adsorption kinetics for  $\beta$ -lactoglobulin fibrils. On the other hand, the interfacial shear rheology showed the formation of a highly elastic interface with the presence of  $\beta$ -lactoglobulin fibrils, and the longer fibrillar structure contributed a higher modulus than the native monomers. Similar results were observed in lysozyme and ovalbumin fibril systems.<sup>89</sup> Moreover, the interfacial behaviours of the  $\beta$ -lactoglobulin fibril system could be influenced by pH value and ionic strength. When the pH was increased to approach the isoelectric point of  $\beta$ -lactoglobulin (e.g. from 2 to 6), both the interfacial storage and loss moduli reached a plateau; with increasing ionic strength, the moduli increased without strain overshoot.<sup>90,91</sup> According to calculations by Jordens *et al.*,<sup>92</sup> the association energy of amyloid fibrils to liquid interfaces is on the order of  $60\,000\ k_B T$ ; this high interfacial affinity leads to excellent stability at liquid/liquid interfaces.

The outstanding interfacial properties and protein-based structures of amyloid fibrils have drawn wide attention in the

food industry to serve as food grade ingredients.<sup>93,94</sup> Serfert *et al.*<sup>93</sup> used fibrillar  $\beta$ -lactoglobulin from whey protein isolate (WPI) and native WPI as an emulsifier to prepare oil/water (O/W) emulsions under acidic conditions for the encapsulation of fish oil. In contrast to native WPI, the WPI fibrils exhibited higher elasticity at the O/W interface and higher microencapsulation efficiency for fish oil. Moreover, the fibrillar structure provided better barrier properties than the native WPI, which led to improved antioxidative effects. Humblet-Hua *et al.*<sup>89</sup> fabricated ovalbumin fibrils hundreds of nanometers in length for stabilizing the O/W interface as a first step; multilayer microcapsules were then prepared by layer-by-layer adsorption of ovalbumin fibrils and high-methoxyl pectin. The release rate of active ingredients obviously decreased with increasing layers of the shell. The amyloid fibrils not only stabilized the O/W emulsion, but also enhanced the emulsion properties under different conditions. Mantovani *et al.*<sup>94</sup> have proven that WPI fibrils can stabilize an O/W emulsion to endure simulated gastric conditions. In contrast, the emulsion stabilized by the native WPI was destabilized in the simulated intestinal conditions. These results suggest the applicability of amyloid fibril-stabilized emulsions in the food industry. In addition to O/W emulsions, biocompatible water-in-water (W/W) emulsions are widely applied in biology, storage and processing of biomolecules and drugs.<sup>95</sup> However, the ultralow interfacial tension of all-aqueous emulsions requires increased size or optimized geometry for surface-active compounds to counteract Brownian motions.<sup>96</sup> Song *et al.*<sup>97</sup> fabricated an all-aqueous emulsion using lysozyme fibrils as the surface-active agent. The diameter of droplets in the emulsion reached dozens of micrometers, and these droplets were covered by two-dimensional cross-linked networks of fibrils. Both the high surface affinity and effective packing at the all-aqueous interfaces of the amyloid fibrils led to stabilization of the W/W emulsions, termed 'fibrillosomes'; this may inspire new strategies to fabricate synthetic vesicles by an all-aqueous process (Fig. 5).

### 3.3 Bio-inspired amyloid-directed surface functionalization

As mentioned above, amyloid fibrils of bacteria and rodlets of hydrophobins enable their adherence to other surfaces; similar functions have also been exhibited in marine sessile crustaceans. Like mussels, barnacles secrete protein-rich

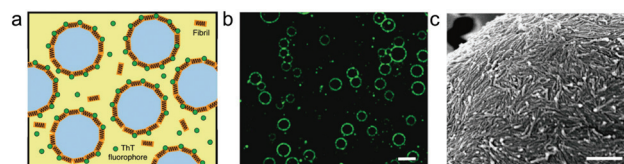


**Fig. 5** (a) Scheme and (b) fluorescence microscopy image of ThT-dyed lysozyme fibrils accumulated at the interface of W/W emulsion droplets. Scale bar =  $20\ \mu\text{m}$ . (c) SEM image confirming that lysozyme fibrils deposit as a monolayer at the emulsion interface. Scale bar =  $500\ \text{nm}$ . (Reproduced from ref. 97 with permission from Nature Publishing Group.)

cements for attachment to foreign surfaces in marine environments. The 3,4-dihydroxyphenylalanine (DOPA) system has been proven to be a key factor in the adhesion of mussels;<sup>98</sup> however, no evidence indicates that the DOPA system is involved in the adhesion of barnacles.<sup>99,100</sup> Although the adhesive mechanism of amyloids has still not been completely elucidated,<sup>50,101</sup> the high aspect ratio structure of amyloids, integrating hydrophobic, electrostatic, and hydrogen-bond interactions and disulphide bonding, should be responsible for the attachment to various surfaces.<sup>102,103</sup> Both the adhesive amyloids in biofilms/barnacles and DOPA from mussels have inspired the development of novel bio-inspired adhesives and materials for surface functionalization.<sup>104</sup> By combining the two natural adhesion systems, Zhong *et al.*<sup>17</sup> used synthetic biology techniques to fabricate two genetic fusion constructs, CsgA-Mfp3 and Mfp5-CsgA, that consisted of Mfp3, Mfp5 (representatives of DOPA-based mussel adhesives originating from *Mytilus galloprovincialis*) and CsgA (the amyloid protein that forms the core component of Curli fibrils). The hybrid peptide could assemble into a fibrillar structure, driven by the amyloid CsgA core, and expose the adhesive Mfp domains. This designed proteinaceous material exhibited strong underwater adhesion strength, reaching  $20.9 \text{ mJ m}^{-2}$ . This synthetic-biology approach was also carried out in the work of Nguyen *et al.*,<sup>105</sup> in which the functional peptide domains were genetically appended to CsgA; this endowed a biofilm of *E. coli* with versatile functions, such as adherence onto specific substrates and nanoparticle templates.

It has been suggested that the amyloid formation of peptides and proteins can be manipulated *in vitro* under relatively extreme conditions, such as acidic pH value, high temperature, high ion strength and organic solvent.<sup>106</sup> Tunable amyloids with rigid, flexible or stacked fibril structures towards various applications are typically obtained after relatively long times (typically tens of hours). In order to simplify the formation of amyloid-based materials for large-scale use and fabricate multifunctional surfaces, a fast and hierarchical amyloid-like assembly strategy was developed by our group; this strategy shed new light on 2D functional amyloids. Our approach is based on a superfast amyloid-like transition of lysozymes in aqueous phase upon treatment with tris(2-carboxyethyl)phosphine (TCEP), a highly efficient disulphide bond (S–S bond) reducing agent, in physiological conditions.<sup>107,108</sup> The breaking of S–S bonds led to a transition from  $\alpha$ -helices to  $\beta$ -sheets and fast phase transition from soluble monomers to insoluble aggregations with intrinsic internal amyloid stacking structures and robust adhesion to surfaces.<sup>109</sup> These aggregations evolved into transparent supramolecular nanofilms at air/water or liquid/solid interfaces and necklace-like microparticles in solution (Fig. 6a).<sup>110</sup> These unique assembled structures are different from conventional amyloid fibrils, which inspired us to explore them for surface functionalization. Firstly, it has been proven that phase-transited lysozymes (PTL) can be steadily immobilized on various substrates, including polymers, oxides and metals; the coated surfaces exhibit moderate hydrophilicity and obvious enhancement of corrosion

resistance.<sup>111</sup> Moreover, the necklace-like microparticles-coated surface exhibits unique features, such as 100% reversible switching between non-fouling and bioconjugation status.<sup>111</sup> Due to the high positive charge of lysozymes, the PTL-coated surfaces exhibited strong electrostatic interactions with anionic compounds. Therefore, a biomimetic lipid membrane was introduced as a mild buffer zone between the PTL-coated surface and anionic giant unilamellar vesicles (GUVs) to suppress the strong coulombic force-induced GUV destruction, which provided a new method for controllable capture/release of batch GUVs on a substrate.<sup>112</sup> Depending on the experimental conditions, the deposition of necklace-like microparticles on substrates endowed materials with hierarchical surface roughnesses, which provided a key condition to achieve bio-based superhydrophobicity. With further chemical grafting of fluoroalkanes to the coating, a stable superhydrophobic surface was obtained with a water contact angle (WCA) of 156 to 168°. Based on this proteinaceous superhydrophobic surface, protein crystallization could be largely accelerated and facilitated due to the strong convergent concentration effect of protein solution droplets on the surface (Fig. 6b).<sup>113</sup>

In addition to the direct deposition of PTL microparticles on the surfaces, nanofilms assembled at air/water or liquid/solid interfaces have drawn increasing attention due to their flexible structures for further processing. Both top-down and bottom-up strategies were carried out for micro/nano-fabrications based on this type of PTL nanofilm, including immobilization of initiator for surface-initiated atom transfer radical polymerization (ATRP), UV and electron beam sensitive green photolithography and patterned electroless deposition of Ag and Cu on flexible polymeric materials directed by abundant active groups from the nanofilm surface ( $-\text{NH}_2$ ,  $-\text{COOH}$ ,  $-\text{OH}$  *et al.*).<sup>108</sup> Lysozymes are functional enzymes that are also widely distributed in nature to catalyse the hydrolysis of microbial cell wall components.<sup>114</sup> Inspired by this property, Yang *et al.* further found that PTL nanofilm-coated materials not only exhibited broad-spectrum antimicrobial action toward Gram-positive/negative bacteria and fungi, but also showed antifouling properties for proteins and platelets. This performance was attributed to the intrinsic triple-combination of positive charges and hydrophobic residues as well as surface hydration effects in the protein nanofilm (Fig. 6c).<sup>115</sup> Recently, a PTL nanofilm was also used as an interfacial template to promote the growth of hydroxyapatite (HAp) film.<sup>116</sup> The functional groups ( $-\text{COOH}$ ,  $-\text{OH}$  *et al.*) on the PTL nanofilm offered abundant chelation sites for  $\text{Ca}^{2+}$  ions, which could then direct the nucleation and growth of bioactive HAp. On the other hand, the adhesion of amyloid-like structures in the PTL nanofilm led to outstanding bonding stability between HAp and substrates such as bone and tooth *in vivo*, which offered a new route for mimicking natural structures and achieving tissue engineering (Fig. 6d).<sup>116</sup> Very recently, the detailed mechanism of the robust adhesion of PTL nanofilms onto versatile material surfaces was systematically investigated.<sup>101</sup> In probably the first experimental study on the interfacial adhesion mechanism of amyloid-like materials, Yang

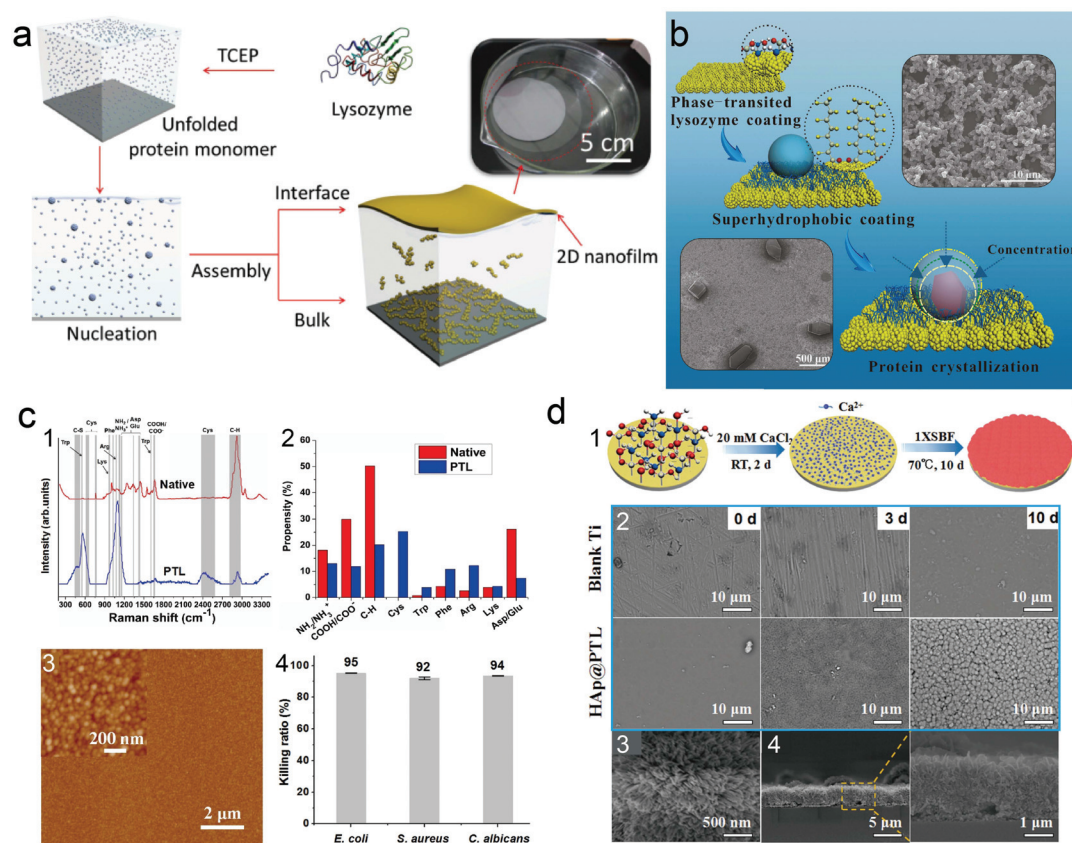


**Fig. 6** (a) Schematic of the proposed mechanism for the formation of nanofilms and necklace-like microparticles (a is reproduced from ref. 110 with permission from Wiley-VCH). (b) Fabrication of a superhydrophobic surface based on phase-transitioned lysozyme microparticle-coated substrates; protein crystallization could be greatly accelerated and facilitated on this superhydrophobic surface (b is reproduced from ref. 113 with permission from Wiley-VCH). (c) A synergistic combination of positive charges and hydrophobic amino acid residues on a nanofilm enhanced its antimicrobial capability: c1: Raman spectra of the PTL nanofilm surface and native lysozyme, in which the characteristic peaks for amino acid residues were used to calculate the propensity; c2: the propensity diagram for typical amino acid residues existing on the PTL nanofilm surface and in the native lysozyme; c3: the typical surface morphology of the PTL nanofilm revealed by AFM; c4: the killing efficiencies of the PTL nanofilm toward *E. coli*, *S. aureus*, and *C. albicans* (c is reproduced from ref. 115 with permission from American Chemical Society). (d) Abundant active groups on the nanofilm enriched the interface, with strong bonding stability to Ca<sup>2+</sup>, and facilitated the formation of HAp both *in vivo* and *in vitro*: d1: the scheme for the PTL nanofilm-assisted HAp crystal formation; d2: typical SEM images showing the effects of the PTL nanofilm modification of the Ti substrate on the formation of HAp minerals at different culture times; d3: high-magnification SEM image showing the formation of a lath-like structure after incubation for 2 weeks; d4: FE-SEM images of a HAp cross-section on the PTL nanofilm after incubation for 2 weeks (d is reproduced from ref. 116 with permission from Wiley-VCH).

*et al.*<sup>101</sup> revealed a novel multiplex bonding model on polar and non-polar abiotic surfaces for amyloid-like protein nanofilms; also, different binding modes for respective material chemical structures, including metal-sulfur coordination bonding, hydrogen bonding, and electrostatic and hydrophobic interactions, and their corresponding bonding strengths were elucidated. These findings provide insight into amyloid adhesion mechanisms and reveal strategies for the theory-driven design of engineered adhesives that harness great promise for advanced materials and devices.

## 4. Conclusions and outlook

In this review, we present the notable functions of amyloids at surfaces/interfaces in both nature and artificial materials.

Amyloids, which have ordered structures, provide a variety of interfacial activities in nature from lower organisms to mammals; this has inspired numerous ideas for the manipulation of interfacial amyloids. Various outstanding studies have proven that amyloids can not only promote surface/interface functions, but that these protein-based motifs also offer excellent biocompatibility and thus enormous opportunity for the food industry, tissue engineering, smart surfaces, *etc.*<sup>15,117</sup> (Fig. 7). On the other hand, amyloids can be readily fabricated using facile methods and inexpensive proteins, which further expands the functional amyloid family for artificial materials.

However, some challenges must still be addressed, such as intensive studies of the mechanisms and behaviours of amyloid assembly and adhesion directed by surfaces/interfaces, developing the applications of oligomers (the non-fibrillar amyloid aggregates at the initial stage of amyloid for-

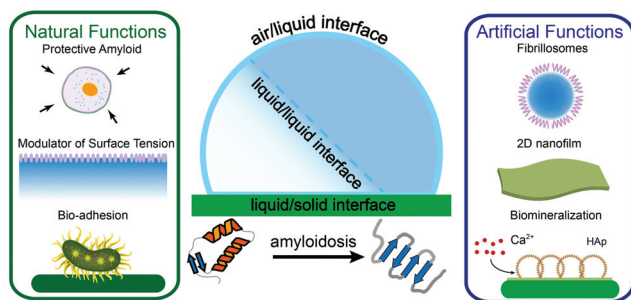


Fig. 7 Brief summary of functional amyloids at surfaces/interfaces in nature and artificial materials.

mation), and surface functionalization of micro/nano-structures. Furthermore, chemical or physical modification of amyloid proteins can offer a novel pathway for surface immobilization of functional compounds. We believe that amyloid materials, with their highly ordered nanostructures and intrinsically proteinaceous features, have great potential in the fields of surface/interface science, nanomaterials, synthetic biology and biomimetics.

## Conflicts of interest

There are no conflicts to declare.

## Acknowledgements

P. Y. acknowledges funding from the National Natural Science Foundation of China (No. 51673112 and 21374057) and the 111 Project (No. B14041). C. L. thanks the Fundamental Research Funds for the Central Universities (2016CBZ005).

## References

- 1 P. Yang and W. Yang, *Chem. Rev.*, 2013, **113**, 5547–5594.
- 2 J. D. Krutty, S. K. Schmitt, P. Gopalan and W. L. Murphy, *Curr. Opin. Biotechnol.*, 2016, **40**, 164–169.
- 3 Y. Zhao, H. M. Wong, S. C. Lui, E. Y. W. Chong, G. Wu, X. Zhao, C. Wang, H. Pan, K. M. C. Cheung, S. Wu, P. K. Chu and K. W. K. Yeung, *ACS Appl. Mater. Interfaces*, 2016, **8**, 3901–3911.
- 4 V. B. Cashin, D. S. Eldridge, A. Yu and D. Zhao, *Environ. Sci.: Water Res. Technol.*, 2018, **4**, 110–128.
- 5 Q. Ye, F. Zhou and W. Liu, *Chem. Soc. Rev.*, 2011, **40**, 4244–4258.
- 6 H. Ejima, J. J. Richardson, K. Liang, J. P. Best, M. P. van Koeverden, G. K. Such, J. Cui and F. Caruso, *Science*, 2013, **341**, 154–157.
- 7 Q. Wei and R. Haag, *Mater. Horiz.*, 2015, **2**, 567–577.
- 8 J. D. Sipe, M. D. Benson, J. N. Buxbaum, S.-i. Ikeda, G. Merlini, M. J. M. Saraiva and P. Westermark, *Amyloid*, 2014, **21**, 221–224.
- 9 R. Riek and D. S. Eisenberg, *Nature*, 2016, **539**, 227–235.
- 10 I. Cherny and E. Gazit, *Angew. Chem., Int. Ed.*, 2008, **47**, 4062–4069.
- 11 S. M. Butterfield and H. A. Lashuel, *Angew. Chem., Int. Ed.*, 2010, **49**, 5628–5654.
- 12 G. Raposo and M. S. Marks, *Traffic*, 2002, **3**, 237–248.
- 13 D. M. Fowler, A. V. Koulov, W. E. Balch and J. W. Kelly, *Trends Biochem. Sci.*, 2007, **32**, 217–224.
- 14 S. K. Maji, D. Schubert, C. Rivier, S. Lee, J. E. Rivier and R. Riek, *PLoS Biol.*, 2008, **6**, e17.
- 15 T. P. J. Knowles and R. Mezzenga, *Adv. Mater.*, 2016, **28**, 6546–6561.
- 16 M. Ahmed, J. Davis, D. Aucoin, T. Sato, S. Ahuja, S. Aimoto, J. I. Elliott, W. E. Van Nostrand and S. O. Smith, *Nat. Struct. Mol. Biol.*, 2010, **17**, 561–567.
- 17 C. Zhong, T. Gurry, A. A. Cheng, J. Downey, Z. Deng, C. M. Stultz and T. K. Lu, *Nat. Nanotechnol.*, 2014, **9**, 858–866.
- 18 V. A. Iconomidou and S. J. Hamdrakas, *Curr. Protein Pept. Sci.*, 2008, **9**, 291–309.
- 19 M. F. B. G. Gebbink, D. Claessen, B. Bouma, L. Dijkhuizen and H. A. B. Wösten, *Nat. Rev. Microbiol.*, 2005, **3**, 333–341.
- 20 V. A. Iconomidou, G. Vriend and S. J. Hamdrakas, *FEBS Lett.*, 2000, **479**, 141–145.
- 21 G. D. Mazur, J. C. Regier and F. C. Kafatos, *Insect Ultrastructure*, Springer Press, Boston, 1982, pp. 150–185.
- 22 S. J. Hamdrakas, J. R. Paulson, G. C. Rodakis and F. C. Kafatos, *Int. J. Biol. Macromol.*, 1983, **5**, 149–153.
- 23 D. C. Benaki, A. Aggeli, G. D. Ghryssikos, Y. D. Yiannopoulos, E. I. Kamitsos, E. Brumley, S. T. Case, N. Boden and S. J. Hamdrakas, *Int. J. Biol. Macromol.*, 1998, **23**, 49–59.
- 24 V. A. Iconomidou, G. Vriend and S. J. Hamdrakas, *FEBS Lett.*, 2000, **479**, 141–145.
- 25 V. A. Iconomidou, G. D. Chryssikos, V. Gionis, A. S. Galanis, P. Cordopatis, A. Hoenger and S. J. Hamdrakas, *J. Struct. Biol.*, 2006, **156**, 480–488.
- 26 V. A. Iconomidou, G. D. Chryssikos, V. Gionis, G. Vriend, A. Hoenger and S. J. Hamdrakas, *FEBS Lett.*, 2001, **499**, 268–273.
- 27 L. Jovine, H. Qi, Z. Williams, E. Litscher and P. M. Wassarman, *Nat. Cell Biol.*, 2002, **4**, 457–461.
- 28 S. Whelly, S. Johnson, J. Powell, C. Borchardt, M. C. Hastert and G. A. Cornwall, *PLoS One*, 2012, **7**, e36394.
- 29 N. Egge, A. Muthusubramanian and G. A. Cornwall, *PLoS One*, 2015, **10**, e0129907.
- 30 N. N. Louros, V. A. Iconomidou, P. Giannelou and S. J. Hamdrakas, *PLoS One*, 2013, **8**, e73258.
- 31 N. N. Louros, E. D. Chryssina, G. E. Baltatzis, E. S. Patsouris, S. J. Hamdrakas and V. A. Iconomidou, *FEBS Lett.*, 2016, **590**, 619–630.
- 32 J. Greenwald, M. P. Friedmann and R. Riek, *Angew. Chem., Int. Ed.*, 2016, **128**, 11781–11785.
- 33 M. B. Linder, G. R. Szilvay, T. Nakari-Setälä and M. E. Penttilä, *FEMS Microbiol. Rev.*, 2005, **29**, 877–896.

- 34 A. B. W. Han, M. A. V. Wetter, L. G. Lugones, H. C. van der Mei, H. J. Wessels and J. G. H. Busscher, *Curr. Biol.*, 1999, **9**, 85.
- 35 N. J. Talbot, M. J. Kershaw, G. E. Wakley, O. De Vries, J. Wessels and J. E. Hamer, *Plant Cell*, 1996, **8**, 985.
- 36 P. Butko, J. P. Buford, J. S. Goodwin, P. A. Stroud, C. L. McCormick and G. C. Cannon, *Biochem. Biophys. Res. Commun.*, 2001, **280**, 212–215.
- 37 A. H. Y. Kwan, R. D. Winefield, M. Sunde, J. M. Matthews, R. G. Haverkamp, M. D. Templeton and J. P. Mackay, *Proc. Natl. Acad. Sci. U. S. A.*, 2006, **103**, 3621–3626.
- 38 M. L. De Vocht, K. Scholtmeijer, E. W. Van Der Vegte, O. M. H. de Vries, N. Sonveaux, H. A. B. Wösten, J. M. Ruyschaert, G. Hadziioannou, J. G. H. Wessels and G. T. Robillard, *Biophys. J.*, 1998, **74**, 2059–2068.
- 39 M. L. De Vocht, I. Reviakine, W. P. Ulrich, W. Bergsma-Schutter, H. A. B. Wösten, H. Vogel, A. Brisson, J. G. H. Wessels and G. T. Robillard, *Protein Sci.*, 2002, **11**, 1199–1205.
- 40 K. Meister, A. Bäumer, G. R. Szilvay, A. Paananen and H. J. Bakker, *J. Phys. Chem. Lett.*, 2016, **7**, 4067–4071.
- 41 M. L. de Vocht, I. Reviakine, H. A. B. Wösten, A. Brisson, J. G. H. Wessels and G. T. Robillard, *J. Biol. Chem.*, 2000, **275**, 28428–28432.
- 42 V. K. Morris, A. H. Kwan and M. Sunde, *J. Mol. Biol.*, 2013, **425**, 244–256.
- 43 A. H. Y. Kwan, R. D. Winefield, M. Sunde, J. M. Matthews, R. G. Haverkamp, M. D. Templeton and J. P. Mackay, *Proc. Natl. Acad. Sci. U. S. A.*, 2006, **103**, 3621–3626.
- 44 A. M. Gravagnuolo, S. Longobardi, A. Luchini, M. S. Appavou, L. D. Stefano, E. Notomista, L. Paduano and P. Giardina, *Biomacromolecules*, 2016, **17**, 954–964.
- 45 M. Bokhove, D. Claessen, W. de Jong, L. Dijkhuizen, E. J. Boekema and G. T. Oostergetel, *J. Struct. Biol.*, 2013, **184**, 301–309.
- 46 D. Claessen, R. Rink, W. de Jong, J. Siebring, P. de Vreugd, F. G. H. Boersma, L. Dijkhuizen and H. A. B. Wösten, *Genes Dev.*, 2003, **17**, 1714–1726.
- 47 H. C. Flemming and J. Wingender, *Nat. Rev. Microbiol.*, 2010, **8**, 623–633.
- 48 M. R. Chapman, L. S. Robinson, J. S. Pinkner, R. Roth, J. Heuser, M. Hammar, S. Normark and S. J. Hultgren, *Science*, 2002, **295**, 851–855.
- 49 A. P. White, D. L. Gibson, S. K. Collinson, P. A. Banser and W. W. Kay, *J. Bacteriol.*, 2003, **185**, 5398–5407.
- 50 E. P. DeBenedictis, J. Liu and S. Keten, *Sci. Adv.*, 2016, **2**, e1600998.
- 51 P. Larsen, J. L. Nielsen, M. S. Dueholm, R. Wetzell, D. Otzen and P. H. Nielsen, *Environ. Microbiol.*, 2007, **9**, 3077–3090.
- 52 L. Song, M. R. Hobaugh, C. Shustak, S. Cheley, H. Bayley and J. E. Gouaux, *Science*, 1996, **274**, 1859–1865.
- 53 C. Corbo, R. Molinaro, M. Tabatabaei, O. C. Farokhzad and M. Mahmoudi, *Biomater. Sci.*, 2017, **5**, 378–387.
- 54 I. Banerjee, R. C. Pangule and R. S. Kane, *Adv. Mater.*, 2011, **23**, 690–718.
- 55 R. Riek and D. S. Eisenberg, *Nature*, 2016, **539**, 227–235.
- 56 C. Aisenbrey, T. Borowik, R. Byström, M. Bokvist, F. Lindström, H. Misiak, M. Sani and G. Gröbner, *Eur. Biophys. J.*, 2008, **37**, 247–255.
- 57 E. Y. Chi, C. Ege, A. Winans, J. Majewski, G. Wu, K. Kjaer and K. Y. C. Lee, *Proteins*, 2008, **72**, 1–24.
- 58 V. N. Uversky, J. Li and A. L. Fink, *J. Biol. Chem.*, 2001, **276**, 44284–44296.
- 59 P. T. Wong, J. A. Schauerte, K. C. Wisser, H. Ding, E. L. Lee, D. G. Steel and A. Gafni, *J. Mol. Biol.*, 2009, **386**, 81–96.
- 60 K. Berthelot, C. Cullin and S. Lecomte, *Biochimie*, 2013, **95**, 12–19.
- 61 H. A. Lashuel, D. Hartley, B. M. Petre, T. Walz and P. T. Lansbury, *Nature*, 2002, **418**, 291–291.
- 62 A. Quist, I. Doudevski, H. Lin, R. Azimova, D. Ng, B. Frangione, B. Kagan, J. Ghiso and R. Lal, *Proc. Natl. Acad. Sci. U. S. A.*, 2005, **102**, 10427–10432.
- 63 S. Rocha, R. Krastev, A. F. Thünemann, M. C. Pereira, H. Möhwald and G. Brezesinski, *ChemPhysChem*, 2005, **6**, 2527–2534.
- 64 L. M. Pandey, S. Le Denmat, D. Delabouglise, F. Bruckert, S. K. Pattanayek and M. Weidenhaupt, *Colloids Surf., B*, 2012, **100**, 69–76.
- 65 A. Keller, M. Fritzsche, Y. P. Yu, Q. Liu, Y. M. Li, M. Dong and F. Besenbacher, *ACS Nano*, 2011, **5**, 2770–2778.
- 66 K. Shezad, K. Zhang, M. Hussain, H. Dong, C. He, X. Gong, X. Xie, J. Zhu and L. Shen, *Langmuir*, 2016, **32**, 8238–8244.
- 67 L. Shen, T. Adachi, D. Vanden Bout and X. Y. Zhu, *J. Am. Chem. Soc.*, 2012, **134**, 14172–14178.
- 68 G. Gao, M. Zhang, P. Lu, G. Guo, D. Wang and T. Sun, *Angew. Chem., Int. Ed.*, 2015, **127**, 2273–2278.
- 69 A. Gupta, T. Sakthivel and S. Seal, *Prog. Mater. Sci.*, 2015, **73**, 44–126.
- 70 D. Losic, L. L. Martin, M. I. Aguilar and D. H. Small, *Pept. Sci.*, 2006, **84**, 519–526.
- 71 F. T. Arce, H. Jang, S. Ramachandran, P. B. Landon, R. Nussinov and R. Lal, *Soft Matter*, 2011, **7**, 5267–5273.
- 72 S. Bag, R. Mitra, S. DasGupta and S. Dasgupta, *J. Phys. Chem. B*, 2017, **121**, 5474–5482.
- 73 P. Nedumpully-Govindan, E. N. Gurzov, P. Chen, E. H. Pilkington, W. J. Stanley, S. A. Litwak, T. P. Davis, P. C. Ke and F. Ding, *Phys. Chem. Chem. Phys.*, 2016, **18**, 94–100.
- 74 M. Mahmoudi, O. Akhavan, M. Ghavami, F. Rezaee and S. M. A. Ghiasi, *Nanoscale*, 2012, **4**, 7322–7325.
- 75 Q. Li, L. Liu, S. Zhang, M. Xu, X. Wang, C. Wang, F. Besenbacher and M. Dong, *Chem. – Eur. J.*, 2014, **20**, 7236–7240.
- 76 L. Baweja, K. Balamurugan, V. Subramanian and A. Dhawan, *J. Mol. Graphics Modell.*, 2015, **61**, 175–185.
- 77 M. Li, A. Zhao, K. Dong, W. Li, J. Ren and X. Qu, *Nano Res.*, 2015, **8**, 3216–3227.

- 78 G. Qing, S. Zhao, Y. Xiong, Z. Lv, F. Jiang, Y. Liu, H. Chen, M. Zhang and T. Sun, *J. Am. Chem. Soc.*, 2014, **136**, 10736–10742.
- 79 T. Frachon, F. Bruckert, Q. Le Masne, E. Monnin and M. Weidenhaupt, *Langmuir*, 2016, **32**, 13009–13019.
- 80 V. K. Morris, Q. Ren, I. Macindoe, A. H. Kwan, N. Byrne and M. Sunde, *J. Biol. Chem.*, 2011, **286**, 15955–15963.
- 81 M. Hoernke, J. A. Falenski, C. Schwieger, B. Kokschi and G. Brezesinski, *Langmuir*, 2011, **27**, 14218–14231.
- 82 S. Campioni, G. Carret, S. Jordens, L. Nicoud, R. Mezzenga and R. Riek, *J. Am. Chem. Soc.*, 2014, **136**, 2866–2875.
- 83 R. J. Green, I. Hopkinson and R. A. L. Jones, *Langmuir*, 1999, **15**, 5102–5110.
- 84 H. Zhu and S. Damodaran, *J. Agric. Food Chem.*, 1994, **42**, 846–855.
- 85 A. L. Campbell, S. D. Stoyanov and V. N. Paunov, *Soft Matter*, 2009, **5**, 1019–1023.
- 86 X. M. Zhou, U. Shimanovich, T. W. Herling, S. Wu, C. M. Dobson, T. P. J. Knowles and S. Perrett, *ACS Nano*, 2015, **9**, 5772–5781.
- 87 U. Shimanovich, I. Efimov, T. O. Mason, P. Flagmeier, A. K. Buell, A. Gedanken, S. Linse, K. S. Åkerfeldt, C. M. Dobson, D. A. Weitz and D. A. Weitz, *ACS Nano*, 2015, **9**, 43–51.
- 88 J. M. Jung, D. Z. Gunes and R. Mezzenga, *Langmuir*, 2010, **26**, 15366–15375.
- 89 K. N. P. Humblet-Hua, G. Scheltens, E. Van Der Linden and L. M. C. Sagis, *Food Hydrocolloids*, 2011, **25**, 569–576.
- 90 P. A. Rühls, N. Scheuble, E. J. Windhab, R. Mezzenga and P. Fischer, *Langmuir*, 2012, **28**, 12536–12543.
- 91 P. A. Rühls, C. Affolter, E. J. Windhab and P. Fischer, *J. Rheol.*, 2013, **57**, 1003–1022.
- 92 S. Jordens, L. Isa, I. Usov and R. Mezzenga, *Nat. Commun.*, 2013, **4**, 1917.
- 93 Y. Serfert, C. Lamprecht, C. P. Tan, J. K. Keppler, E. Appel, F. J. Rossier-Miranda, K. Schroen, R. M. Boom, S. Gorb, C. Selhuber-Unkel, S. Drusch and K. Schwarz, *J. Food Eng.*, 2014, **143**, 53–61.
- 94 R. A. Mantovani, A. C. Pinheiro, A. A. Vicente and R. L. Cunha, *Food Res. Int.*, 2017, **99**, 790–798.
- 95 E. Edmond and A. G. Ogston, *Biochem. J.*, 1968, **109**, 569–576.
- 96 B. T. Nguyen, T. Nicolai and L. Benyahia, *Langmuir*, 2013, **29**, 10658–10664.
- 97 Y. Song, U. Shimanovich, T. C. T. Michaels, Q. Ma, J. Li, T. P. J. Knowles and H. C. Shum, *Nat. Commun.*, 2016, **7**, 12934.
- 98 Q. Ye, F. Zhou and W. Liu, *Chem. Soc. Rev.*, 2011, **40**, 4244–4258.
- 99 M. Nakano and K. Kamino, *Biochemistry*, 2015, **54**, 826–835.
- 100 D. K. Burden, D. E. Barlow, C. M. Spillmann, B. Orihuela, D. Rittschof, R. K. Everett and K. J. Wahl, *Langmuir*, 2012, **28**, 13364–13372.
- 101 J. Gu, S. Miao, Z. Yan and P. Yang, *Colloid Interface Sci. Commun.*, 2018, **22**, 42–48.
- 102 K. Kamino, K. Inoue, T. Maruyama, N. Takamatsu, S. Harayama and Y. Shizuri, *J. Biol. Chem.*, 2000, **275**, 27360–27365.
- 103 G. H. Dickinson, I. E. Vega, K. J. Wahl, B. Orihuela, V. Beyley, E. N. Rodriguez, R. K. Everett, J. Bonaventura and D. Rittschof, *J. Exp. Biol.*, 2009, **212**, 3499–3510.
- 104 C. E. Brubaker and P. B. Messersmith, *Langmuir*, 2012, **28**, 2200–2205.
- 105 P. Q. Nguyen, Z. Botyanszki, P. K. R. Tay and N. S. Joshi, *Nat. Commun.*, 2014, **5**, 4945.
- 106 O. G. Jones and R. Mezzenga, *Soft Matter*, 2012, **8**, 876–895.
- 107 P. Yang, *Macromol. Biosci.*, 2012, **12**, 1053–1059.
- 108 F. Tao, Q. Han, K. Liu and P. Yang, *Angew. Chem., Int. Ed.*, 2017, **56**, 13440–13444.
- 109 C. Li, L. Xu, Y. Zuo and P. Yang, *Biomater. Sci.*, 2018, DOI: 10.1039/C8BM00066B.
- 110 D. Wang, Y. Ha, J. Gu, Q. Li, L. Zhang and P. Yang, *Adv. Mater.*, 2016, **28**, 7414–7423.
- 111 Z. F. Wu and P. Yang, *Adv. Mater. Interfaces*, 2015, **2**, 1400401.
- 112 D. Wang, Z. Wu, A. Gao, W. Zhang, C. Kang, Q. Tao and P. Yang, *Soft Matter*, 2015, **11**, 3094–3099.
- 113 A. Gao, Q. Wu, D. Wang, Y. Ha, Z. Chen and P. Yang, *Adv. Mater.*, 2016, **28**, 579–587.
- 114 H. R. Ibrahim, A. Kato and K. Kobayashi, *J. Agric. Food Chem.*, 1991, **39**, 2077–2082.
- 115 J. Gu, Y. Su, P. Liu, P. Li and P. Yang, *ACS Appl. Mater. Interfaces*, 2016, **9**, 198–210.
- 116 Y. Ha, J. Yang, F. Tao, Q. Wu, Y. Song, H. Wang, X. Zhang and P. Yang, *Adv. Funct. Mater.*, 2018, **28**, 1704476.
- 117 D. M. Ridgley, B. G. Freedman, P. W. Lee and J. R. Barone, *Biomater. Sci.*, 2014, **2**, 560–566.